This is a repository copy of *Study of deposition parameters for the fabrication of ZnO thin films using femtosecond laser*.

White Rose Research Online URL for this paper:
http://eprints.whiterose.ac.uk/104962/

Version: Accepted Version

Study of deposition parameters for the fabrication of ZnO thin films using femtosecond laser

Jaweria Zartaj Hashmi[1,2,*], Khurram Siraj[1], Anwar Latif[1], Mathew Murray[2], Gin Jose[2]

1. Laser and Optronics Centre, Department of Physics, University of Engineering and Technology, Lahore–54890 Pakistan.

2. Applied Photon Science, School of Chemical and Process Engineering, University of Leeds, Leeds LS2 9JT, UK.

*Corresponding Author

Ms. Jaweria Zartaj Hashmi, Assistant Professor,

Laser and Optronics Centre, Department of Physics, University of Engineering & Technology, Lahore–54890, PAKISTAN.

Tel: +92-42-99029204

e-mail: jaweria04@gmail.com

Abstract

Femtosecond (fs) pulsed laser deposition (fs-PLD) of ZnO thin film on borosilicate glass substrates is reported in this work. The effect of important fs-PLD parameters like target-substrate distance, laser pulse energy, and substrate temperature on structure, morphology, optical transparency and luminescence of as deposited films is discussed. XRD analysis reveals that all the films grown using the laser energy range 120 µJ to 230 µJ are polycrystalline when they are deposited at room temperature in a ~ 10^{-5} Torr vacuum. Introducing 0.7 mTorr oxygen pressure, the films show preferred c-axis growth and transforms into a single crystal like film when the substrate temperature is increased to 100 ℃. The Scanning Electron Micrographs show the presence of small nano size grains at 25 ℃, which grow in size to the regular hexagonal shape particles at 100 ℃. Optical transmission of the ZnO film is found to increase with an increase in crystal quality. Maximum transmittance of 95% in the wavelength range 400-1400 nm is achieved for films deposited at 100 ℃ employing a laser pulse energy of 180 µJ. The luminescence spectra show a strong UV emission band peaked at 377 nm close to the ZnO band gap. The shallow donor defects increase at higher pulse energies and higher substrate temperatures, which give rise to violet-blue luminescence. The results indicate that nanocrystalline ZnO thin films with high crystalline quality and optical transparency can be fabricated by using pulses from fs lasers.

Keywords: PLD, femtosecond, crystalline, SEM, optical band gap, luminescence.

1. Introduction

ZnO is a wide band gap semiconductor that is widely studied for its use in transparent electronics [1-2]. in addition to its wide band gap (3.37 eV), ZnO also has a large exciton binding energy (60 meV) and high optical transparency (> 80% for films of thickness ~500 nm) in the ultraviolet (UV)-visible light wavelengths which contribute to expanding the range of ZnO applications from UV lasers and diodes to bio sensors [3], gas sensors [4], piezoelectric sensors [5] and transducers [6]. Microstructure is a key factor which decides the electrical and optical properties of ZnO; that is why ZnO is grown and studied in a variety of forms, e.g. bulk, thin films and nano- crystalline [7]. Several evaporation and sputtering deposition techniques have been employed to achieve highly crystalline and very low roughness (<10nm) ZnO thin films [8] which are basic requirements for optical devices.

PLD has been used as one of the evaporation techniques, where a nano- or femtosecond lasers are employed to produce plasma from the ZnO bulk target material in the presence of some background gas, typically oxygen, and then deposited on a nearby substrate. Laser pulse energy, pulse repetition rate, pulse duration, target-substrate distance, substrate temperature, ambient gas and pressure are all fundamental parameters which on adjustment can lead to desired properties of thin films [9]. Most of the previous studies report use of nanosecond pulsed lasers to produce ZnO crystalline thin films with dense columnar growth and a smooth surface morphology [10-13]. Despite these advantages, the formation of molten droplets and ejection of larger particulates from the target surface hamper efforts to grow ZnO thin films with required optical properties [14].

In pulsed laser deposition of thin films, the laser-matter interaction time determines the target material ablation dynamics. The time should be small enough to suppress the energy dissipation beyond the ablated volume, which is hard to achieve with nanosecond lasers. Nanosecond lasers increase the heat affected zone which leads to damage, segregation of different components in the target [15], ejection of molten droplets and micrometer-sized particles at thin film surface during PLD. Therefore it is expected that these issues related to nanosecond laser ablation can be largely addressed by using fs laser pulses of the order of 100-150 femtoseconds [9]. Okoshi et al. [16] and Millon et al. [17] have pioneered some substantial work on growing ZnO thin films using femtosecond lasers with pulse durations of 130 and 90 femtoseconds but film quality achieved was not as good as in the case of nanosecond PLD. Perriere et al. reported a comparison of nanosecond and femtosecond laser ablation on the ZnO films [18]; and Klini et al. extensively studied the plume dynamics [19] to comment on the smaller particles, higher mosaicity and roughness in ZnO thin films. It was concluded from these works that higher expansion velocities of plasma species produced by ultrashort lasers as compared to nanosecond lasers is the key factor behind this decline of crystallinity. In the previously reported work in fs laser pulse regime, substrate temperature, post deposition annealing, laser pulse energy, deposition time, and oxygen pressure were studied [20-21]. It was observed that high values of laser energies ranging from 1 to 10 mJ were used.

In the present work, lower values of laser pulse energy (ranging from 120 to 230 μJ) and higher value of oxygen pressure (P_{O2} = 0.7 mTorr) as compared to previously reported work are studied for the fabrication of good quality crystalline thin films. Besides energy, the effect of target-substrate distance and substrate temperature are also investigated.

Experiment

A target for PLD of ZnO was made by sintering the cold pressed pellet of 99.9% pure ZnO powder (Alfa Aesar). This target material was ablated by a Ti:sapphire femtosecond laser (wavelength = 800 nm, pulse repetition rate = 1 kHz and pulse duration = 100 fs) to deposit ZnO thin films on borosilicate glass substrates ($3 \times 2 \times 0.1$ cm^3). The borosilicate substrates were cleaned using ethanol and acetone. The target and substrate were rotated continuously at a constant speed of 40 rpm and 20 rpm, respectively during the deposition.

Three series of ZnO thin films samples were prepared by varying the target-to-substrate distance, laser energy and substrate temperature to study the effect of deposition parameters on the characteristics of the films. In a first series of samples the target-substrate distance was varied from 60 mm to 80 mm while the energy was kept constant at 180 µJ. In the second series, the target-substrate distance was fixed at 80 mm while the laser energy incident upon the target was varied from 120 µJ to 230 µJ. In both these series, the substrate was kept at 25 ℃ and the chamber was evacuated down to 10^{-5} Torr. Finally, the substrate temperature was varied from 25 ℃ to 150 ℃ in a 0.7 mTorr oxygen atmosphere. The details of experimental conditions and sample identity for each series are reported in Table 1.

The crystallography of the as-deposited films is characterized using X-ray diffraction (Model: Philips X'Pert MPD) data. Surface morphology is studied using scanning electron microscopy (Model: Hitachi SU8230). Optical transmittance and the ZnO optical band gap energy are obtained from measurements using UV/VIS/NIR spectrophotometer (Model:

PERKIN ELMER Lambda 950). Photoluminescence spectra was acquired from an Edinburgh Instruments FLS920 spectrophotometer at an excitation wavelength of 350-600 nm.

3. Results and Discussion

3.1 X-ray Diffraction

X-ray diffraction spectra of ZnO thin films prepared at different deposition conditions are shown in Fig. 1 and the various crystal parameters obtained from the XRD data is reported in Table 2. Figure 1a shows the diffraction pattern of ZnO thin films deposited at different target-substrate distance whereas Fig. 1b shows the diffraction pattern of ZnO thin films deposited at different laser pulse energies. Three major crystal planes (100), (002) and (101) are observed in the XRD spectra of all the thin films showing their polycrystalline nature. The 2θ values match well with the standard Ref: ICDD No. 00-036-1451. The texture coefficient (TC) illustrates the preferred orientation of the crystals in films and is calculated for all samples using Equation 1

$$TC_{hkl} \ = \frac{I_{hkl}/I_{hkl}^{o}}{\frac{1}{n}\sum_{n} I_{hkl}/I_{hkl}^{o}} \tag{1}$$

where TC_{hkl} is the texture coefficient of the plane (hkl), I_{hkl} is the intensity of the peak corresponding to (hkl) plane of the thin film, I^{o}_{hkl} is the intensity of the (hkl) plane of a polycrystalline standard sample and 'n' is the number of peaks taken into account [22]. TC_{hkl} value of unity represents the plane without preferred orientation whereas TC_{hkl} values higher than unity represent a preferentially grown plane. For calculating texture

coefficient of ZnO thin films, standard intensities from ICDD No. 00-036-1451 are used and the values are reported in Table 2. The TC values are greater than unity for (002) plane and therefore this is the direction of preferred orientation for all samples where the values are obtained. From the analysis of XRD data, laser pulse energy 180 µJ and target-substrate distance 80 mm is selected to deposit the films at different substrate temperatures in the presence of 0.7 mTorr O_2 pressure.

Figure 1c shows the XRD spectra of ZnO thin films T25, T50, T100 and T150. It is evident from the Fig. 1c that high intensity (002) plane preferentially grows in all thin films. The (002) peaks become intense if the substrate temperature is increased from 25 to 150 ℃. The presence of strong c-axis texture (TC ~ 2.28 to 2.97) suggests that the microstructure of the films is changing from polycrystalline to single crystal like when the temperature is increased.

To investigate the effect of deposition parameters on ZnO lattice dimensions, the lattice parameters 'a' and 'c' of hexagonal ZnO are calculated using Equation 2 [23].

$$\frac{1}{d^2} = \frac{4}{3}\left(\frac{h^2+hk+k^2}{a^2}\right) + \frac{l^2}{c^2} \tag{2}$$

Here d is spacing between planes and h, k, l are the Miller indices of these planes. Angular positions (2θ) at (100) and (002) planes and h, k and l values of these planes are used to calculate 'a' and 'c' respectively. These values of 'a' and 'c' are used for calculation of cell volume V ($V = 0.866\ a^2c$) and are reported in Table 2. The lattice constants calculated for ZnO thin films are in good agreement with that of the standard ones for bulk ZnO (a = 3.2498 Å and c = 5.2066 Å). A small increase in the unit cell volume (46.8 to 47.5 Å^3) for

samples H60, H70 and H80 indicates the expansion of ZnO lattice with increase in distance. By increasing the laser pulse energy from 120 µJ to 230 µJ, a random but small variation is observed in cell volume. On the other hand, variation of substrate temperature from 25 to 150 ℃ has reduced the cell volume from 48.6 to 47.3 Å^3 which is close to the standard cell volume of ZnO lattice. This suggests that ZnO lattice dimensions shows dependence on the three fabrication parameters, target to substrate distance, laser energy and temperature.

The unit cells arranged along one plane give rise to the crystallite formation in a crystalline structure. The crystallite size is affected by the growth modes of thin films and plays an important role in defining the optical properties of the films. The average crystallite sizes of all the ZnO thin films are calculated using Scherrer calculator in X'Pert Highscore software. Table 2 shows that crystallite size is reduced from 47 nm to 23 nm when distance between target and substrate is increased from 60 to 80 mm but there is no clear trend with laser energy. The crystallite size of samples T25, T50, T100 and T150 show direct dependence on substrate temperature. The smallest size of 10 nm is observed for sample T25 where this value increases to 49 nm for sample T100. At higher substrate temperatures, nucleation and grain growth is supported by thermal energy which reduces the grain boundaries and increases the average crystallite size. Decrease in unit cell volume and increase in crystallite size at 150 ℃ indicate a change in density of the particles forming nanocrystalline ZnO thin films.

Variations observed in the lattice dimensions and small crystallite size show presence of various stresses in the ZnO thin films. The stress which is parallel to film surface is

calculated using biaxial strain model, according to which the stress parallel to the film surface is proportional to strain perpendicular (c-axis) to film surface. Strain along c-axis is calculated from the values of lattice constant c_{film} and c_{bulk} (ϵ = c_{film}-c_{bulk} / c_{bulk}) and is used in Equation 3 to calculate stress.

$$\sigma = -\ 233 \times 10^9\ \epsilon \tag{3}$$

here σ is the residual stress and ϵ is the strain caused by this stress. The negative values of σ show that ZnO films are under tensile stress while positive sign indicates the presence of compressive stress. It can be seen from Table 2 that compressive stresses are found in the films only when the films are grown at lowest laser pulse energy (E120) or when the substrate temperature is low (T25 and T50). Tensile stress is present in the rest of samples.

From the analysis of different structural parameters given in Table 2, it is found that the variation in d_{TS}, E_l and T_s affect the crystalline growth of ZnO thin films using femtosecond laser deposition. The required crystallite size and film texture can be achieved by carefully selecting these parameters. A comparison of best textured films is presented in Fig. 1d. Three films are deposited at target substrate distance of 80 mm, laser pulse energy 180 µJ and oxygen ambient of 0.7 mTorr. The substrate temperature and deposition time are adjusted to get nearly single-crystal like films. First film is deposited at 25 °C for deposition time (t_D) of three hours, second film is deposited at 100 °C for one hour, an d third film is deposited at 150 °C for one hour. All the samples exhibit c-axis growth of ZnO thin f ilms. Peak shape (height, intensity and broadening) represents quality of crystalline structure. From the 002 peak analysis, it is concluded that the substrate temperature affects the film

growth more strongly as compared to the deposition time. So it is suggested from the analysis that for the deposition of highly crystalline c-axis oriented thin films, d_{TS}, E_l, T_s and t_D should be taken as 80 mm, 180 µJ, 150 °C and 1 hour respectively in the presence of oxygen pressure of 0.7 mTorr.

3.2 Scanning Electron Microscopy

Surface morphology of ZnO thin films deposited under different deposition conditions is studied using scanning electron micrographs given in Fig. 2. All these thin films are deposited at constant target-substrate distance (80 mm) and laser pulse energy (180 µJ). Figure 2a shows image of ZnO thin film deposited at 25 °C in vacuum. Small nano-size grains are observed having non-uniform size distribution over the whole film surface. Presence of large size spherical cluster made up of smaller grains is also visible. This represents qualitatively rough surface of ZnO thin film. Figure 2b represents micrographs of ZnO thin films deposited at 25 °C in the presence of 0.7 mT orr O_2. Cluster formation is reduced in the presence of background gas. By increasing substrate temperature to 50 °C, uniform distribution of small grains is observed acco mpanied by agglomerated clusters as shown in Fig. 2c. Figure 2d shows that increasing the substrate temperature to 100 °C has considerably improved the surface morphology as uniformly distributed hexagonal ZnO grains (average size < 65 nm) are making up the surface of thin film. Further increase in T_s to 150 °C results in the diffusion of grains as visible grain boundaries has been reduced (Fig. 2e). This is because the thermal energy gained by atoms from substrate aids the atomic diffusion and grain growth along favorable sites in the lattice. When the temperature was 100 °C, this thermal energy supporte d the growth

of hexagonal ZnO nanocrystals but further increase in temperature supports diffusion and therefore spherical grains are observed. To observe the effect of deposition time, micrograph of ZnO thin film deposited at 25 ℃ for 3 hours is shown in Fig. 2f. Smooth and uniform film surface is obtained which is characterized by the presence of dense grain growth with no visible voids or porosity.

3.3 UV/VIS Spectrophotometry

Optical transmittance and corresponding optical band gap values of ZnO thin films grown at different deposition conditions is shown in Fig. 3. Figure 3a shows the optical transmission of samples H60, H70 and H80. It is evident that the placement of substrate at different distances from the target affects the transmission spectra of ZnO thin films. The optical transmittance (%T) increases from 57 % to 70 % with increase in d_{TS} from 60 mm to 80 mm respectively. Moreover, the UV-transmission edge shifts to lower wavelengths (≈ 400 nm) when the d_{TS} is increased to 80 mm.

The optical transmission spectra of samples E120, E150, E180, E200 and E230 is shown in Fig. 3b. It can be seen that the transmission of light through ZnO thin films decreases down to 50 % with the increase in E_l except for 180 µJ. The maximum transmittance of 70% is achieved for sample E180. The plasma plume of ZnO contains the neutral zinc, Zn^+ and neutral oxygen. The presence of more neutral species and high density of metallic elements give rise to the metallic luster that blocks most of the light from transmission, instead it is reflected. By varying the distance and the energy, apparent change in the ratio of dark to transparent area on the film surface is observed as shown in Fig. 3h. Consequently, a change in transmittance spectra is also observed. The spatial distribution of energy in plasma plume follows the Gaussian profile. So the most energetic

species are present in the center while those with lower energy are at outer edges of plume. The kinetic energy is a function of mass and velocity so the lighter particles (electrons) are at the front whereas the massive ones (ions and neutral) are behind the lighter ones. As oxygen has less mass as compared to the zinc atoms so the oxygen atoms are easily displaced from their mean paths through inelastic collisions as compared to Zn. The formation of dark region in the center of thin film suggests accumulation of such Zn atoms and lack of ZnO at this point.

Transmittance spectra of ZnO thin films T25, T50, T100 and T150 is given in Fig. 3c. The introduction of oxygen as background gas minimizes the non-stoichiometry of elements (Zn and O) in the films. Figure 3c confirms this point, where the transmittance of ZnO thin film, deposited in the presence of 0.7 mTorr O_2 has increased to 90 %. It is observed that the average transmittance in the visible and near infra-red region of electromagnetic spectrum changes with change in T_s but the transmission edge remains sharp and almost at same wavelength for all films. At first the %T decreases from 90% to 75 % by increasing the temperature from 25 ℃ to 50 ℃, and then increases to 95 % when T_s increases to 100 ℃. Further increase in T_s to 150 ℃ reduces the transmission of light to 85 %. These results can be described on the basis of the SEM analysis where it was observed that background gas helps to reduce the qualitative roughness and defects whereas the substrate temperature improves stoichiometric and uniform film deposition, providing sufficient thermal energy to adatoms for the film growth. This uniformity is also confirmed by the absence of any darker regions in the films with $T_s \leq 100$ °C whereas beyond this temperature range, uniformity is disturbed which reduces transmittance at 150 ℃.

Absorbance (A) of ZnO thin films deposited at different deposition conditions is calculated from A = 2 - $\log_{10}$ (%T), derived from Beer's law. These absorbance values are used to estimate the optical band gap energy (E_g) by plotting $(A \times h\nu)^2$ versus photon energy ($h\nu$) known as Tauc's curve. The extrapolation of linear portion of Tauc's curves to photon energy axis gives value of optical band gap energy [24]. The E_g values of ZnO thin films obtained from Tauc's curve are plotted as a function of target-substrate distance, laser pulse energy and substrate temperature in Fig. 3d, e and f respectively. The E_g in Fig. 3d varies from 3.1 to 3.09 eV with variation in d_{TS}. As this variation is very small (0.01 eV) so it is negligible. But Fig. 3e suggests a strong dependence of E_g on E_l, where it varies randomly from 2.92 eV (E150) to maximum of 3.11 eV (E180). The reduction in E_g of ZnO thin film from the E_g of bulk (3.37 eV) indicates presence of some defect states closer to the conduction band or valence band. This might be due to the structural disorder or defects which can serve as scattering points. The presence of nanocrystallites from XRD analysis (Table 2) and the large number of grain boundaries resulting from smaller grain size in SEM micrographs (Fig. 2) confirm the existence of defects. The disturbed stoichiometry can also be another reason.

It is evident from Fig. 3f that the values of E_g as a function of substrate temperature are comparatively closer to E_g of bulk ZnO. Highest value of 3.36 eV is obtained for sample T25. This suggests an improvement in stoichiometry and reduction in relevant structural defects as compared to other ZnO thin films. With increase in T_s from 25 to 50 ℃, E_g decreases to 3.26 eV. This reduction in E_g is due to the presence of clusters and smaller grain sizes at surface of thin films. As the grain size and shapes improve with increase in T_s to 150 ℃, the E_g also increases.

Besides structural defects like grain size and grain boundaries, stacking faults are also significant when the thickness of the thin film increases. As thickness affects the optical band gap, therefore, the thickness of the thin films deposited at different values of T_s is measured using spectroscopic ellipsometer and is given in Fig. 3g. Thickness increases linearly from 29 to 77 nm with T_s. This increase in thickness means more number of ZnO layers will be deposited at higher substrate temperatures. Thus stacking faults will also increase, which are responsible for the low values of E_g at higher T_s.

3.4 Photoluminescence

Photoluminescence (PL) spectroscopy is used to investigate the optical properties of ZnO thin films. The luminescence spectra depends on the structure, chemical composition, intrinsic and extrinsic defects like vacancies, interstitials and impurities respectively [25]. As these factors relies on the deposition parameters and film growth modes, therefore the PL spectra of all three series of ZnO thin films is shown in Fig. 4 a, b and c. A strong UV emission band is observed at ≈ 377 nm (3.29 eV) in Fig. 4a corresponding to near band edge emission in ZnO and is pretty close to the band gap value of bulk ZnO. Generally two emission bands are reported and discussed in the PL spectra of ZnO: a UV and a visible emission [11, 26-27]. The UV emission of ZnO at room temperature is attributed to the combination of two emissions in which one is related to free exciton recombination and other is related to free electron-to-acceptor recombination [28] whereas the visible emission is a result of deep level impurities. The absence of any strong visible emission in PL spectra can be due to the absence of these deep level impurities. Peak intensity and FWHM of the UV emission band varies for samples and H60 has the strongest PL. The FWHM (line broadening) of the PL emission band is 11.8

14

nm, 12.5 nm and 13.1 nm for samples H60, H70 and H80 respectively. This reflects that the UV emission of ZnO thin films is strongly affected by the position of substrate with respect to the target in fs-PLD.

Fig. 4b shows that the intensity of UV emission band centered at 377 nm, increases with increase in E_l from 120 to 150 µJ and then decreases when E_l is increased further to 230 µJ. Also two new broad band emissions centering at 422 nm and 439 nm and a shoulder at 474 nm are observed for sample E230. Emission band at 422 nm is assigned to the electron-hole recombination between Zn interstitial and valence band [26]. The 439 nm (2.82 eV) and 474 nm (2.62 eV) reveals the presence of some other defect state near conduction band, acting as a shallow donor levels responsible for a radiative transition between electron from this level to the top of valence band [20].The appearance of 422 and 439 nm band is ascribed to the formation of Zn rich films because zinc interstitial (Zn_i) generates a shallow donor level. Presence of Zn_i is due to the absence of oxygen background during deposition and the use of higher E_l of 230 µJ which scatters the light mass oxygen atoms as compared to heavier zinc atoms. Introduction of oxygen environment should remove this type of defect. This explanation is further confirmed by Fig. 4c where the PL spectrum of sample T25 does not show any violet-blue emission.

Increasing the substrate temperature from 25 to 100 °C, the intensity of UV emission also increases. A small red shift in the emission wavelength from 377 to 381 nm is also observed. The smallest FWHM of UV peak is also observed for T100, reflecting the strongest UV emission from ZnO thin film. The increase in intensity of UV peak and red shift is due to the increasing grain size [29] with increase in substrate temperature. Further increase in T_s to 150 °C not only reduces the intensity of UV emission at 381 nm

but also new emission bands are observed at 413, 443 and 456 nm. These violet and blue emissions can be assigned to different defect states (Zn_i, Zn_i^{++} etc.) present near the conduction band [30]. Inset of Fig. 4c shows photoluminescence spectra of ZnO deposited at 25 °C for 3 h. The emission band comprises only UV luminescence and is very broad, which shows poor UV emission when the deposition time is increased from 1 hour to 3 hours.

Conclusions

From the analysis of XRD, SEM, UV/VIS and PL spectroscopy of ZnO thin films deposited using various deposition parameters of ultrashort laser deposition, it is concluded that microstructure is the key factor on which the optical transmittance and UV emission of ZnO depends. This microstructure can be controlled by selecting the suitable values of target-substrate distance, laser pulse energy and substrate temperature, when employing PLD for thin film deposition. The qualitative roughness which is a measure of size distribution and the defects are reduced by using lower values of laser energy (180 µJ) and substrate temperature of 100 °C in this experiment. Also instead of d eposition time, substrate temperature is much more effective in controlling film optical (?) quality.

Acknowledgements:

References

(1)   Huiyong Liu, V. Avrutin, N. Izyumskaya, U. Ozgur, H. Morkoc, Superlattice Microst 48, 458 (2010).

(2)   U¨ mit O¨ zgu¨r, Daniel Hofstetter, Hadis Morkoc, Proceedings of the IEEE 98, 1255 (2010).

(3)   S. K. Aryaa, S. Sahab, J. E. Ramirez-Vickc, V. Guptab, S Bhansalid, S. P. Singhe, Anal Chim Acta 737, 1 (2012).

(4)   O. Lupan, L. Chow, S. Shishiyanu, E. Monaico, T. Shishiyanu, V. S¸ontea, B. Roldan Cuenya, A. Naitabdi, S. Park, A. Schulte, Mater Res Bull 44, 63 (2009).

(5)   E. Lee, J. Park, M. Yim, Y. Kim, G. Yoon, Appl Phys Lett 106, 1 (2015).

(6)   Q. F. Zhou, C. Sharp, J. M. Cannata, K. K. Shung, G. H. Feng, E. S. Kim, Appl Phys Lett 90, 113502 (2007).

(7)   Shubra Singh, P. Thiyagarajan, K. M. Kant, D. Anita, S. Thirupathiah, N. Rama, B. Tiwari, M. Kottaisamy, M. S. Ramachandra Rao, J Phys D Appl Phys 40, 6312 (2007).

(8)   R. Kumar, G. Kumar, O. Al-Dossary, A. Umar, Mater. Express 5, 1 (2015).

(9)   J. Perriere, E. Millon, V. Craciun, in Pulsed Laser Deposition of Thin Films: Applications-Led Growth of Functional Materials, ed. By R. Eason (Willey, 2007, New Jersey), p. 261.

(10)   V. Craciun, J. Elders, J. G. E. Gardeniers, Ian W. Boyd, Appl Phys Lett 65, 5 (1994).

(11)   Seong-Jun Kang, Hyun-Ho, Yung-Sup Yoon, J Korean Phys Soc 1, 183 (2007).

(12)   M.G. Tsoutsouvaa, C.N. Panagopoulos, D. Papadimitriou, I. Fasaki, M. Kompitsas, Mat Sci Eng B-Solid 176, 480 (2011).

(13)   M. Gupta, F. Rezwana Chowdhury, D. Barlage, Y. Yin Tsui, Appl Phys A-Mater 110, 793 (2013).

(14)   A. Ohtomo, A. Tsukazaki, Semicond Sci Tech 20, S1 (2005).

(15)   D. Bäuerle, Laser Processing and Chemistry, 4th edn. (Springer-Verlag, Berlin, 2011), pp. 489-492.

(16)   M. Okoshi, K. Higashikawa, M. Hanabusa, Appl Surf Sci 154–155, 424 (2000).

(17)   E. Millon, O. Albert, J. C. Loulergue, J. Etchepare, D. Hulin, W. Seiler, J. Perrière, J Appl Phys 88, 6937 (2000).

(18)   J. Perrière, E. Millon, W. Seiler, C. Boulmer-Leborgne, V. Craciun, O. Albert, J. C. Loulergue, J. Etchepare, J Appl Phys 91, 690 (2002).

(19)   A. Klini, A. Manousaki, D. Anglos, and C. Fotakis, J Appl Phys 98, 123301 (2005).

(20)   Y. Yang, H. Long, G. Yang, A. Chen, Q. Zheng, P. Lu, Vacuum 83, 892 (2009).

(21)   J. Lik Hang Chau, Min-Chieh Yang, T. Nakamura, S. Sato, Chih-Chao Yang, Chung-Wei Cheng, Opt Laser Technol 42, 1337 (2010).

(22)   H. Faiz, K. Siraj, M. S. Rafique, S. Naseem, A. W. Anwar, Indian J Phys 89, 353 (2015).

(23)   O. Lupan, T. Pauporte, L. Chow, B. Viana, F. Pelle, L. K. Ono, B. Roldan Cuenya, H. Heinrich, Appl Surf Sci 256, 1895 (2010).

(24)   R. Pérez-Casero, A. Gutiérrez-Llorente, O. Pons-Y-Moll, Wilfrid, R. Marie Defourneau, D. Defourneau, E. Millon, J. Perrière, P. Goldner, B. Viana, J Appl Phys 97, 054905 (2005).

(25)   G. Kaur, A. Mitra, K.L. Yadav, Progress In Natural Science: Materials International 25, 12 (2015).

(26)   P. K. Samanta, S. K. Patra, A. Ghosh, P. Roy. Chaudhuri, Inter.J. of Nanoscience and Nanotechnology 1, 81 (2009).

(27)   M. Ramani, S. Ponnusamy, C. Muthamizhchelvan, Opt Mater 34, 817 (2012).

(28)   Y. M. Lu, X. P.Li, P. J. Cao, S. C. Su, F. Jia, S. Han, W. J. Liu, D. L. Zhu, X. C. Ma, J. of Spectroscopy 1, 1 (2013).

(29)   H. J. Chang, C. Z. Lu, Y. Wang, Chang-Sik Son, Seong-Il Kim, Young-Hwan Kim, In-Hoon Choi, J Korean Phys Soc 45, 959 (2004).

(30)   K. Bandopadhyay, J. Mitra, RSC Adv. 5, 23540 (2015).

List of Figures

Fig. 1 XRD spectrum of ZnO thin films deposited at different deposition conditions. (a) Variation of target-substrate distance, (b) variation of laser energy, (c) variation of substrate temperature and (d) comparison of deposition time and temperature

Fig. 2 SEM micrographs of selected ZnO thin films deposited for 1 h in vacuum at (a) 25 °C. Deposition for 1h in ambient oxygen at (b) 25 °C (c) 50 °C (d) 100 °C and (e) 150 °C, whereas (f) represents deposition at 25 °C in the presence of O_2 for 3 h
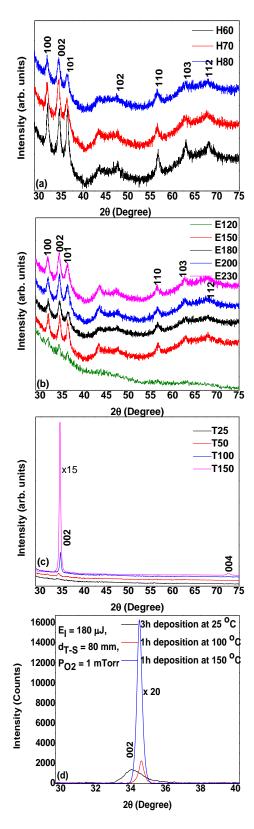
Fig. 3 Transmittance (T %) and optical band gap energy of ZnO thin films deposited by varying substrate distance from the target, laser energy and substrate temperature. Inset of (d) shows Tauc plot for the estimation of optical band gap energy while (g) shows effect of substrate temperature on the thickness of films which is obtained from spectroscopic ellipsometer and (h) shows images of two thin films deposited at 230 µJ and 120 µJ respectively

Fig. 4 Photoluminescence spectra of ZnO thin films deposited by varying (a) target-substrate distance, (b) laser energy and (c) substrate temperature
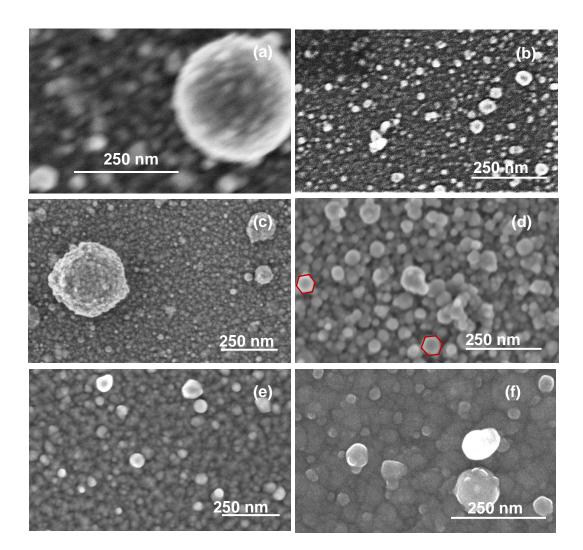
List of Tables

Table 1 Experimental details of ZnO thin films prepared by varying different PLD parameters
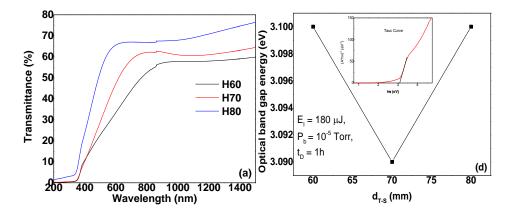
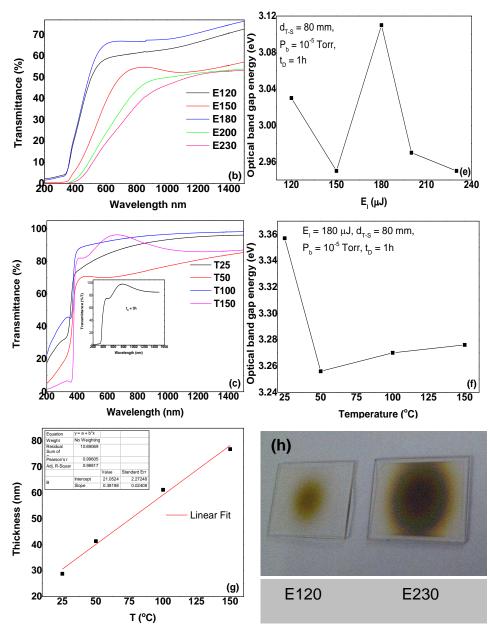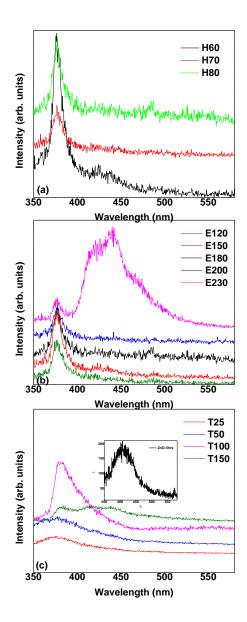**Table 2** Structural parameters calculated from XRD spectrum

Fig.1

Fig.2

Fig. 3

Fig. 4

Table 1

Sample Series	Sample Identity	Target-substrate distance (mm)	Laser pulse energy (μJ)	Substrate temperature (℃)	Ambient environment/ Pressure (Torr)
Series-I	H60	60	180	25	Air / 10^{-5}
	H70	70	180	25	Air / 10^{-5}
	H80	80	180	25	Air / 10^{-5}
Series-II	E120	80	120	25	Air / 10^{-5}
	E150	80	150	25	Air / 10^{-5}
	E180	80	180	25	Air / 10^{-5}
	E200	80	200	25	Air / 10^{-5}
	E230	80	230	25	Air / 10^{-5}
Series-III	T25	80	180	25	O_2 / 0.7×10^{-3}
	T50	80	180	50	O_2 / 0.7×10^{-3}
	T100	80	180	100	O_2 / 0.7×10^{-3}
	T150	80	180	150	O_2 / 0.7×10^{-3}

Table 2

Sample Name	Lattice constant		Cell Volume V (Å)³	Crystallite size nm	Stress GPa	Degree of texture		
	a (Å)	c (Å)				100	002	101
H60	3.2300	5.1791	46.8	46	1.79	1.05	1.32	0.63
H70	3.2416	5.2129	47.4	26	0.28	0.96	1.59	0.48
H80	3.2457	5.2115	47.5	23	0.35	0.99	1.56	0.42
E120	3.2532	5.2260	47.9	15	-0.30	1.02	1.44	0.57
E150	3.2453	5.2025	47.4	31	0.75	0.96	1.41	0.54
E180	3.2457	5.2115	47.5	23	0.35	0.99	1.56	0.42
E200	3.2489	5.2023	47.5	26	0.76	0.93	1.53	0.54
E230	3.2595	5.2193	48.0	19	0.01	0.9	1.56	0.54
T25	3.2654	5.2693	48.6	10	-2.23	0.72	2.28	---
T50	3.2675	5.2369	48.4	17	-0.78	0.66	2.28	---
T100	----	5.1787	----	49	1.81	---	---	---
T150	3.2397	5.2001	47.3	47	0.86	0.006	2.97	0.009